Dalton Transactions

COMMUNICATION

View Article Online
View Journal | View Issue

Cite this: *Dalton Trans.*, 2014, **43**, 5269

Received 6th November 2013,
Accepted 19th December 2013

DOI: 10.1039/c3dt53141d

www.rsc.org/dalton

Turn-on trivalent cation selective chemodosimetric probe to image native cellular iron pools†

M. Venkateswarulu,[a] Trinetra Mukherjee,[b] Subhrakanti Mukherjee[b] and Rik Rani Koner*[a]

A new turn-on cell permeable chemodosimetric probe 1 has been developed and its application in the selective detection of trivalent cations (Fe^{3+}/Cr^{3+}/Al^{3+}) at a sub-nanomolar level has been demonstrated. The selectivity of 1 over a broad spectrum of mono- and divalent metal ions was established using fluorescence spectroscopy. Moreover, the changes in the absorption spectra of 1 in the presence of trivalent cations enabled the most bio-relevant metal ion Fe^{3+} over Cr^{3+}/Al^{3+} to be distinguished. The probe was found to be successful in the fluorescence imaging of native cellular iron pools. The fluorescence imaging of the native iron pools of banana pith further supported the high sensitivity of 1 towards Fe^{3+} present in living systems. To the best of our knowledge, this is the first example of a turn-on chemodosimetric probe to image native cellular Fe^{3+} pools.

The importance of iron, the most abundant transition metal in biological systems, in monitoring various biological events has been well investigated and documented in the literature.[1] The concentration of iron in a living system has been found to be crucial for the smooth functioning of biological processes. Iron dishomeostasis (either deficiency or overload) may cause certain cancers and dysfunction of various organs.[1–6] A fluorescence bioimaging technique has been adapted as one of the most sensitive and efficient techniques for imaging intracellular labile or free metal ions.[1c,7–18] Often this technique provides valuable information related to cell biology such as the dynamic changes of these metal ions in the cellular environment, their role in regulating various cellular processes, *etc.*[8,9] In the last few decades, though a large number of fluorescence chemosensors have been developed by various research groups for the efficient detection of Fe^{3+} in environmental samples, chemosensors for the detection of iron in biological samples are much fewer in number.[19] Moreover, molecular probes that detect/image native cellular iron pools have been rarely reported.[1a] The main reasons for this scarcity of such probes are their cell impermeability, lack of sensitivity and lack of solubility in aqueous or semi-aqueous solutions. In addition to these, and due to its strong paramagnetic quenching nature, the development of a turn-on fluorescence chemosensing agent for Fe^{3+} has always been a challenging task. Therefore, there is a need to develop a cell permeable turn-on molecular sensor for Fe^{3+} having potential in imaging native cellular iron pools.

Often, in recent times, chemodosimeters have been preferred over chemosensors for the fluorescence bioimaging of various analytes including anions, small- and bio-molecules due to their high selectivity, sensitivity and rapid response time.[20] The basic difference between a chemosensor and a chemodosimeter is that the binding interaction between the chemosensor and analyte which renders a fluorescence signal is non-covalent and reversible, whereas chemodosimeters interact with the analytes through an irreversible chemical reaction. While a large number of chemosensors have been reported over the years for imaging a wide range of analytes in biological samples, Li and coworkers in their most recent review mentioned that the number of chemodosimeters reported to date is only around 200.[20] Also, the carefully documented examples in this review clearly demonstrate the strong potential of chemodosimeters in luminescent bioimaging.[20] Though few chemodosimeters have been reported in recent times as fluorescence bioimaging agents for various metal ions, only one innovatively designed chemodosimetric probe has been reported to date which has potential in imaging overloaded Fe^{3+} in living cells.[21] Similarly, two recent reports have described the development of fluorescent probes for imaging labile Fe^{2+} pools in living cells.[22] However, to the best of our knowledge, no chemodosimetric probe has been reported to date for the imaging of native cellular Fe^{3+} pools.

A recent report from the Costero group carefully demonstrated the importance of a trivalent cations sensor.[23] Though very few chemosensors have been reported to date for the selective detection of trivalent cations,[24] no chemodosimetric

[a]*School of Basic Sciences, Indian Institute of Technology Mandi, Mandi-175001, H.P., India. E-mail: rik@iitmandi.ac.in; Fax: +91-1905-237924; Tel: +91-1905-237994*
[b]*Department of Microbiology, Burdwan University, Burdwan, West Bengal, India*
† Electronic supplementary information (ESI) available. See DOI: 10.1039/c3dt53141d

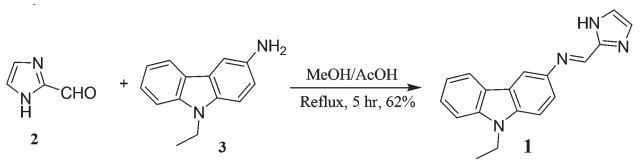

Scheme 1 Synthesis of chemodosimetric probe **1**.

probe has yet been reported to selectively detect trivalent cations over mono- and divalent cations.

Herein, we report our recent development of an imine-based turn-on chemodosimetric probe for the selective detection of trivalent cations at a sub-nanomolar level and its application in the fluorescence imaging of native cellular iron pools.

The chemodosimetric probe **1** (Scheme 1) was synthesized by the condensation of 2-imidazolecarboxaldehyde, **2** and 3-amino-*N*-ethyl carbazole, **3** in methanol.

The desired product was isolated as a yellow solid and characterized using FT-IR, $^{1}H/^{13}C$ NMR and high resolution mass spectroscopy (Fig. S1 and S2†). Various spectroscopic techniques were used to investigate the chemodosimetric nature of probe **1** against several metal ions. A combination of THF–H_2O (8 : 2 v/v) was used as the solvent system to study the absorption and emission properties of **1**. Initially, probe **1** (10 μM) showed two absorption bands centered at 295 nm (ε = 23 700, high-energy absorption band) and at 350 nm (ε = 18 400, low energy band) (Fig. S3†). These two bands arose mainly due to the π–π* and n–π* transitions of aromatic rings and the imine (C═N) bond, respectively. Whereas the addition of Fe^{3+} (0–360 μM) to a solution of **1** (10 μM) resulted in a significant increase in intensity of the high-energy band at 295 nm, no change in intensity of the high-energy band was observed upon the addition of Al^{3+}/Cr^{3+} (Fig. S4†). The presence of trivalent cations caused a disappearance of the low energy band at 350 nm indicating cleavage of the imine bond (Fig. S4†). These spectral changes efficiently distinguished Fe^{3+} over Al^{3+}/Cr^{3+}. UV-vis spectra in other solvent combinations were also recorded and are reported in the ESI (S4b–d†).

Interestingly, when these experiments were performed in THF, no such changes in the absorption spectra of **1** were observed (Fig. S5†). This indicates that water played a major role in causing the changes in the absorption spectra of **1** in the presence of trivalent cations and we speculate that such changes occurred due to trivalent cation mediated hydrolysis of the imine-bond resulting in the generation of amine and aldehyde. To further prove this, control experiments were performed using pure aldehyde and amine in the presence of trivalent cations. We observed that the absorption spectra of the carbazole amine in the presence of trivalent cations were similar to that of **1** in the presence of trivalent cations in a mixture of THF–H_2O (8 : 2) (Fig. S6†). These experimental results revealed that the strong Lewis acidity of trivalent cations ($Fe^{+3}/Al^{+3}/Cr^{+3}$) over other metal ions facilitated the hydrolytic cleavage of the imine-bond (Scheme S2†).[25–27]

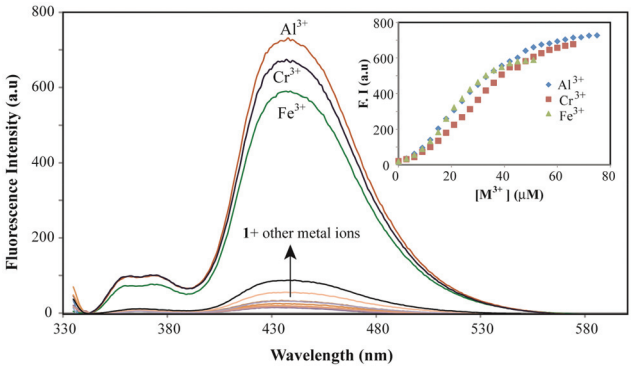

Fig. 1 Emission spectra of compound **1** (1 μM), and **1** in the presence of different metal ions (51 μM, 75 μM, 63 μM for $Fe^{3+}/Al^{3+}/Cr^{3+}$, respectively, and 100 μM for the other cations) in a THF–H_2O (8 : 2) mixture, (λ_{ex} = 330 nm, λ_{em} = 430 nm). Inset: fluorescence intensity as a function of $Fe^{3+}/Cr^{3+}/Al^{3+}$ concentration.

Next we investigated the fluorescence response of **1** when treated with $Fe^{3+}/Al^{3+}/Cr^{3+}$ in a mixture of THF–H_2O (8 : 2). The fluorescence titrations of **1** in the presence and absence of the trivalent cations were performed to examine the cleavage of the imine-bond. As shown in Fig. 1, **1** (1 μM) itself was found to be weakly fluorescent upon excitation at 330 nm. The weak fluorescence of the probe was mainly due to a combination of *E*/*Z* isomerization and photoinduced electron transfer (PET) from the imidazole unit to the fluorophore carbazole.[28,29] Upon the addition of $Fe^{+3}/Al^{+3}/Cr^{+3}$ (51 μM, 75 μM, 63 μM, respectively), probe **1** (1 μM) exhibited a remarkable enhancement in fluorescent intensity at 430 nm. However, the other metal ions showed no such effect when **1** was excited at 330 nm in identical conditions (Fig. 1).

In order to understand the origin of such turn-on fluorescence of **1** in the presence of $Fe^{3+}/Al^{3+}/Cr^{3+}$, and based on the experimental data that we obtained during absorption studies, the fluorescence spectra of **3** were recorded in identical conditions. The carbazole amine **3** showed fluorescence emission at 430 nm when excited at 330 nm and the emission spectrum was similar to that of the emission spectra of **1** (Fig. S7†). This supported our conclusion that the fluorescence enhancement was due to the hydrolysis of the imine-bond and formation of carbazole amine **3**.

To confirm this further, experiments were performed using THF as the solvent and in the absence of water (Fig. S8†), no such changes in the emission spectra of **1** in the presence of $Fe^{3+}/Al^{3+}/Cr^{3+}$ were observed. The above spectral studies suggest that the presence of water was one of the key factors in cleaving the imine-bond. All these experimental data infer that **1** could be used as a chemodosimetric probe to detect trivalent cations in environmental systems.

In order to support the hydrolytic cleavage of the imine linkage, ^{1}H-NMR titration experiments were performed using Al^{3+} as the model trivalent cation (in order to avoid peak broadening in the presence of Fe^{3+}/Cr^{3+} due to their paramagnetic nature) in a mixture of solvents DMSO-d_6–D_2O (8 : 2) (Fig. S9†). In the absence of Al^{3+}, the imine proton appeared at

8.60 ppm. Upon the addition of Al^{+3} to the same solution, a new peak at 9.60 ppm appeared which could be attributed to the aldehydic proton of 2-imidazolecarboxaldehyde **2**. Over time the intensity of the signal for the imine proton slowly decreased and an almost complete disappearance of the imine peak was observed after a few minutes of addition of Al^{3+}.

Similarly, the mass spectra of **1** in the presence of the trivalent cations showed the disappearance of the molecular ion peak for **1** (289.14) and the distinct appearance of peaks corresponding to the aldehyde and amine (97.18 and 211.38, respectively) (Fig. S10†). These results fully support the irreversible binding of a trivalent cation to **1** followed by the hydrolytic cleavage of the imine linkage.

Using the (3 sigma/slope) method, the limit of detection was calculated and found to be in a sub-nanomolar range.[30] The present probe **1** could detect as low as 0.38, 0.38 and 0.36 nM of Fe^{3+}, Al^{3+} and Cr^{3+}, respectively (Fig. S11a–c†).

Competition experiments were performed to investigate the potential of **1** as a selective chemodosimeter for $Fe^{3+}/Al^{3+}/Cr^{3+}$. The addition of an excess amount (102 μM) of a large number of various mono- and divalent metal ions including biologically active and heavy metal ions (nitrate salts of Na^{+}, Ag^{+}, Mg^{2+}, Pb^{2+}, Cd^{2+}, Ni^{2+}, Co^{2+}, Zn^{2+} and Cu^{2+}; and the chloride salt of Hg^{2+}, sulfate salt of Fe^{2+} were used) to a solution of **1** in THF–H_2O (8 : 2) did not result in any enhancement in fluorescence, whereas the addition of $Fe^{3+}/Cr^{3+}/Al^{3+}$ (51 μM, 63 μM and 75 μM respectively) to the same solution resulted in an increase in fluorescence intensity (Fig. 2). It is worth mentioning that Fe^{2+} showed no effect on the emission spectra of **1** under identical experimental conditions and a high selectivity for Fe^{3+} over Fe^{2+} was observed (Fig. 2). These results strongly support our conclusion that **1** could be used as an $Al^{3+}/Cr^{3+}/Fe^{3+}$ selective 'turn-on' chemodosimeter.

The probe was found to be stable within a pH range of 5.6–10 (Fig. S12a†). To check the working pH range for probe **1**, pH dependent studies were performed and the probe was found to work efficiently within a pH range 6.8–7.2 (Fig. S12b†).

To gain insight into the hydrolysis kinetics of probe **1**, we investigated the time dependent changes in the fluorescence intensity of **1** in the presence of trivalent cations. Though the hydrolysis of **1** started immediately after the addition of the trivalent cations, the maximum fluorescence emission intensity was observed within 10 minutes after the addition of the trivalent cations (Fig. S13a–e†).

Given the utmost biological importance of Fe^{3+}, and considering the probe's selectivity for Fe^{3+} over all other metal ions present in biological milieu, as well as its efficacy in detecting iron in a sub-nanomolar level, we became interested in investigating the potential of **1** to image native cellular iron pools. *Candida albicans* cells (IMTECH no. 3018) from an exponentially growing culture in a potato dextrose broth (pH 5.2, incubation temperature 37 °C) were collected by centrifugation at 3000 rpm for 5 minutes. Next, these cells were thoroughly washed twice by suspending them in a 0.1 M HEPES buffer (pH 7.2) followed by centrifugation at the same speed as above. One set of washed cells was treated with an EDTA solution to chelate the native cellular labile/free iron pools and then the cells were treated with probe **1** (50 μM). Another set of washed cells was incubated separately with probe **1** (50 μM) for 30 minutes without any EDTA treatment and washed two times. A third set of washed cells was overloaded with Fe^{3+} (1 mM) by treating with $FeCl_3$ for 30 minutes, washed and finally treated with **1** for another 30 minutes. Finally, the treated cells were mounted on a grease free glass slide and observed under a Leica DM 1000 Fluorescence microscope with a UV filter. Cells treated with EDTA followed by **1** were used as the control (Fig. 3a). The cells treated with probe **1** showed a strong blue emission indicating imaging of the native cellular iron pool (Fig. 3b). To prove this further, when

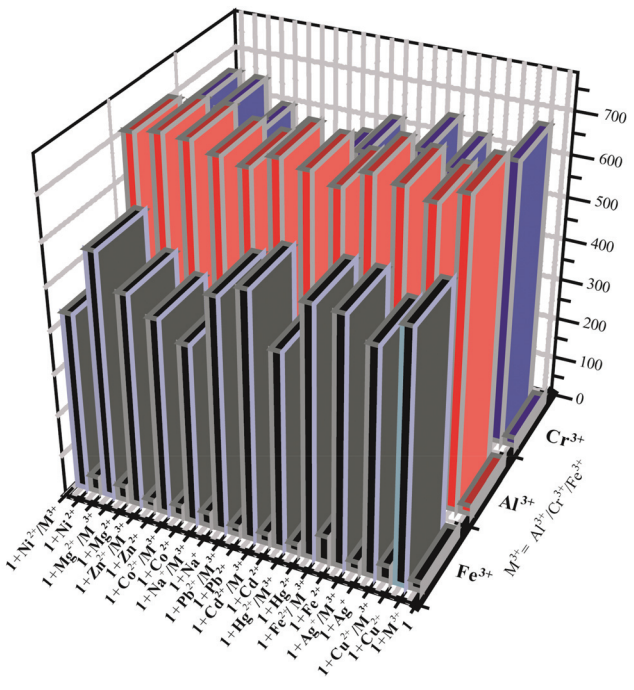

Fig. 2 Fluorescence response of **1** (1 μM) towards $Fe^{3+}/Cr^{3+}/Al^{3+}$ (51 μM, 63 μM and 75 μM, respectively) in the presence of excess amounts of (102 μM) various metal ions in THF–H_2O 8 : 2 mixture (λ_{ex} = 330 nm, λ_{em} = 430 nm).

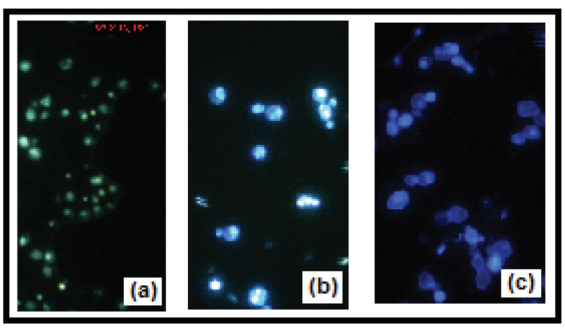

Fig. 3 Fluorescence microscopic photographs of (a) *Candida albicans* cells treated with EDTA followed by probe **1**, (b) *C. albicans* cells treated with **1**, (c) *C. albicans* cells treated with $FeCl_3$ followed by **1**.

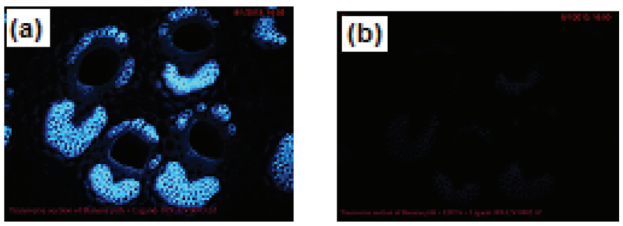

Fig. 4 Fluorescence microscopic photograph of transverse section of (a) banana pith treated with **1**, (b) banana pith treated with EDTA, first, followed by **1**.

the Fe^{3+} overloaded cells were treated with probe **1**, a highly intense emission was observed indicating the presence of a higher concentration of iron which in fact catalyzed the cleavage process more efficiently (Fig. 3c). Therefore, the present chemodosimetric probe **1** could be used for the fluorescence imaging of native cellular iron pools.

The strong potential of **1** in the fluorescence imaging of native iron pools in biological systems was proved further using a plant system. When banana pith sections, as an iron-rich part of the banana plant, were treated with **1**, a strong blue emission was observed indicating imaging of the native iron pools (Fig. 4a). EDTA treated banana pith was used as the control (Fig. 4b).

To conclude, we have demonstrated the synthesis and application of a new turn-on cell permeable chemodosimetric probe for the selective detection of trivalent cations. The limit of detection was so low as to be at a sub-nanomolar level. The probe showed a high selectivity for Fe^{3+} over Fe^{2+} as well as a broad spectrum of other mono- and divalent cations. The probe successfully showed its potential in the fluorescence imaging of native cellular iron pools, being the first chemodosimeter of this kind to do so.

Acknowledgements

Financial support from the Department of Science and Technology (DST), India (grant no. SR/FT/CS 57/2010(G)) is thankfully acknowledged. R. R. K. is thankful to IIT-Mandi for her fellowship. M. V. is grateful to IIT Mandi for his fellowship. We thankfully acknowledge the Director, IIT-Mandi, for research facilities. We are grateful to the Advance Material Research Centre, IIT-Mandi, for their sophisticated instrument facilities. We also gratefully acknowledge the support of USIC (Burdwan University) for the fluorescence microscope facility. We thankfully acknowledge the reviewers for their valuable comments.

References

1 (*a*) Y. Wei, Z. Aydin, Y. Zhang, Z. Liu and M. Guo, *ChemBioChem*, 2012, **13**, 1569; (*b*) H. Glickstein, R. B. Ei, M. Shvartsman and Z. L. Cabantchik, *Blood*, 2005, **106**, 3242; (*c*) F. Petrat, U. Rauen and H. D. Groot, *Hepatology*, 1999, **29**, 1171.
2 E. R. Stadtman, *Annu. Rev. Biochem.*, 1993, **62**, 797.
3 *Inorganic Biochemistry of Iron Metabolism*, ed. R. Crichton, Wiley, Chichester, 2nd edn, 2001, pp. 17–48.
4 T. Rouault, *Nat. Chem. Biol.*, 2006, **2**, 406.
5 B. R. Bacon and R. S. Britton, *Hepatology*, 1990, **11**, 127.
6 D. B. Kell, *BMC Med. Genomics*, 2009, **2**, 2.
7 B. P. Espósito, S. Epsztejn, W. Breuer and Z. I. Cabantchik, *Anal. Biochem.*, 2002, **304**, 1.
8 (*a*) D. W. Domaille, E. L. Que and C. J. Chang, *Nat. Chem. Biol.*, 2008, **4**, 168; (*b*) G. Sivaraman, T. Anand and D. Chellappa, *Analyst*, 2012, **137**, 5881; (*c*) G. Sivaraman, T. Anand and D. Chellappa, *RSC Adv.*, 2013, **3**, 17029.
9 E. M. Nolan and S. J. Lippard, *Acc. Chem. Res.*, 2009, **42**, 193.
10 E. L. Que, D. W. Domaille and C. J. Chang, *Chem. Rev.*, 2008, **108**, 1517.
11 Z. Zhou, M. Yu, H. Yang, K. Huang, F. Li, T. Yi and C. Huang, *Chem. Commun.*, 2008, 338.
12 K. Huang, H. Yang, Z. Zhou, M. Yu, F. Li, X. Gao, T. Yi and C. Huang, *Org. Lett.*, 2008, **10**, 2557.
13 M. Zhang, Y. Gao, M. Li, M. Yu, F. Li, L. Li, M. Zhu, J. Zhang, T. Yia and C. Huang, *Tetrahedron Lett.*, 2007, **48**, 3709.
14 G. Sivaraman and D. Chellappa, *J. Mater. Chem. B*, 2013, **1**, 5768.
15 G. Sivaraman, T. Anand and D. Chellappa, *RSC Adv.*, 2012, **2**, 10605.
16 Z. Dai, L. Tian, Y. Xiao, Z. Ye, R. Zhang and J. Yuan, *J. Mater. Chem. B*, 2013, **1**, 924.
17 L. Tian, Z. Dai, L. Zhang, R. Zhang, Z. Ye, J. Wu, D. Jin and J. Yuan, *Nanoscale*, 2012, **4**, 3551.
18 X. Liu, Z. Ye, W. Wei, Y. Du, J. Yuan and D. Ma, *Chem. Commun.*, 2011, **47**, 8139.
19 (*a*) B. Wang, J. Hai, Z. Liu, Q. Wang, Z. Yang and S. Sun, *Angew. Chem., Int. Ed.*, 2010, **49**, 4576–4579; (*b*) Z. Yang, M. She, B. Yin, J. Cui, Y. Zhang, W. Sun, J. Li and Z. Shi, *J. Org. Chem.*, 2012, **77**, 1143–1147; (*c*) W. Chen, W. Gong, Z. Ye, Y. Lina and G. Ning, *Dalton Trans.*, 2013, **42**, 10093; (*d*) N. R. Chereddy, S. Thennarasu and A. B. Mandal, *Analyst*, 2013, **138**, 1334–1337; (*e*) S. Sen, S. Sarkar, B. Chattopadhyay, A. Moirangthem, A. Basu, K. Dhara and P. Chattopadhyay, *Analyst*, 2012, **137**, 3335; (*f*) Z. Hu, Y. Feng, H. Huang, L. Ding, X. Wang, C. Lin, M. Li and C. Ma, *Sens. Actuators, B*, 2011, **156**, 428; (*g*) S. Wang, X. Meng and M. Zhu, *Tetrahedron Lett.*, 2011, **52**, 2840; (*h*) M. Kumar, R. Kumar, V. Bhalla, P. J. Sharma, T. Kaur and Y. Qurishi, *Dalton Trans.*, 2012, **41**, 408; (*i*) L. Zhang, J. Wang, J. Fan, K. Guo and X. Peng, *Bioorg. Med. Chem. Lett.*, 2011, **21**, 5413–5416; (*j*) G. Sivaraman, V. Sathiyaraja and D. Chellappa, *J. Lumin.*, 2014, **145**, 480; (*k*) S. K. Sahoo, D. Sharma, R. K. Bera, G. Crisponi and J. F. Collan, *Chem. Soc. Rev.*, 2012, **41**, 7195.

20 Y. Yang, Q. Zhao, W. Feng and F. Li, *Chem. Rev.*, 2013, **113**, 192.
21 M. H. Lee, T. V. Giap, S. H. Kim, Y. H. Lee, C. Kang and J. S. Kim, *Chem. Commun.*, 2010, **46**, 1407.
22 (*a*) H. Y. A-Yeung, J. Chan, T. Chantarojsiri and C. J. Chang, *J. Am. Chem. Soc.*, 2013, **135**, 15165; (*b*) T. Hirayama, K. Okuda and H. Nagasawa, *Chem. Sci.*, 2013, **4**, 1250.
23 A. Barba-Bon, A. M. Costero, S. Gil, M. Parra, J. Soto, R. Martínez-Màñez and F. Sancenón, *Chem. Commun.*, 2012, **48**, 3000.
24 (*a*) D. O. Kirsanov, A. V. Legin, V. A. Babain and Yu. G. Vlasov, *Russ. J. Appl. Chem.*, 2005, **78**, 568; (*b*) A. V. Legin, D. O. Kirsanov, V. A. Babain, A. V. Borovoy and R. S. Herbst, *Anal. Chim. Acta*, 2006, **572**, 243; (*c*) M. Venkateswarulu, S. Sinha, J. Mathew and R. R. Koner, *Tetrahedron Lett.*, 2013, **54**, 4683.
25 (*a*) W. Lin, L. Yuan, J. Feng and X. Cao, *Eur. J. Org. Chem.*, 2008, 2689; (*b*) J. A. Dean, *Lange's Handbook of Chemistry*, McGraw-Hill, New York, 13th edn, (section 5), 1987; (*c*) D. V. Prabhu and N. B. Laxmeshwar, *Asian J. Chem.*, 1997, **9**, 70–74; (*d*) V. G. Machado, M. G. Nascimento and M. C. Rezende, *J. Braz. Chem. Soc.*, 1993, **4**, 76–79.
26 N. P. Sadler, C.-C. Chuang and R. M. Milburn, *Inorg. Chem.*, 1995, **34**, 402.
27 V. Lykourinou-Tibbs, A. Ercan and L.-J. Ming, *Catal. Commun.*, 2003, **4**, 549.
28 Y.-D. Cao, Q.-Y. Zheng, C.-F. Chen and Z.-T. Huang, *Tetrahedron Lett.*, 2003, **44**, 4751.
29 N. Saleh, Y. A. Al-Soud and W. M. Nau, *Spectrochim. Acta, Part A*, 2008, **71**, 818.
30 G. L. Long and G. D. Winefordner, *Anal. Chem.*, 1983, **55**, 712A.